N89-25179

ROBUST COMPUTER-AIDED SYNTHESIS AND OPTIMIZATION OF LINEAR MULTIVARIABLE CONTROL SYSTEMS WITH VARYING PLANT DYNAMICS VIA AUTOCON

C.P. LEFKOWITZ, J.A. TEKAWY, P.K. PUJARA
NORTHROP CORPORATION, AIRCRAFT DIVISION
HAWTHORNE, CALIFORNIA

and

M.G. SAFONOV
UNIVERSITY OF SOUTHERN CALIFORNIA
LOS ANGELES, CALIFORNIA

INTRODUCTION

AUTOCON is an automated computer-aided design tool for the synthesis and optimization of linear multivariable control systems based upon user-defined control parameter optimization. Violations in stability and performance requirements are computed from constraints on Single Input/Single Output (SISO) open- and closed-loop transfer function frequency responses, and from constraints on the singular-value frequency responses of Multiple Input/Multiple Output (MIMO) transfer functions, for all critical plant variations. Optimum nonlinear programming algorithms are used in the search for local constrained solutions in which violations in stability and performance are caused either to vanish or be minimized for a proper selection of the control parameters. Classical control system stability and performance design can, in this way, be combined with modern multivariable robustness methods to offer general frequency response loop-shaping via a computer-aided design tool. Complete Nichols, Nyquist, Bode, singular-value Bode magnitude and transient response plots are produced, including user-defined boundary responses. AUTOCON is used to synthesize and optimize the lateral/directional flight control system for a typical high-performance aircraft. (See figure 1.)

- Automated Computer-Aided Workbench Design Tool For Synthesis And Optimization Of Linear Multivariable Control Systems
  - Parameter Optimization Determines Local Constrained Optimal Solutions In Which Violations In User-Specified Stability/Performance Requirements Either Vanish Or Are Minimized
  - Frequency-Domain Loop Shaping Via Nonlinear Mathematical Programming
  - Synthesis/Optimization Considers Each Stability Loop And Constrained Transfer Function For All Plant Variations Simultaneously.
  - User-Defined Control System Architecture, Parameters, Stability Loops, Constrained Transfer Functions
  - Fixed and Varying Plant Dynamics
  - Classical Specs : Stability Margins, Bandwidth, Damping, Overshoot, etc.
  - Sensitivity Analysis

Figure 1

CLASSICAL CONTROL SYSTEM SYNTHESIS AND OPTIMIZATION

The "classical" version of AUTOCON (ref. 1) performs synthesis and optimization of linear control systems using nonlinear mathematical programming (NMP). Stability constraints (stability margins using Nyquist single-loop-at-a-time methods) and system performance constraints for scalar transfer functions are user-specified as are the system architecture and control parameters. Actual system open- and closed-loop frequency responses (airframe plus control system) are computed for the user-specified "initial system" for each stability-loop and constrained closed-loop transfer function, and for all selected plant variations. Similarly, desired and boundary responses are computed from the system requirements. Violations in the actual responses when compared with the desired and boundary responses at each frequency computed (considering all responses simultaneously) are caused either to vanish or are minimized by a proper selection (automated) of the control parameters (parameter optimization). A multivariable control system diagram and stability/performance constraints are depicted in figure 2 below.

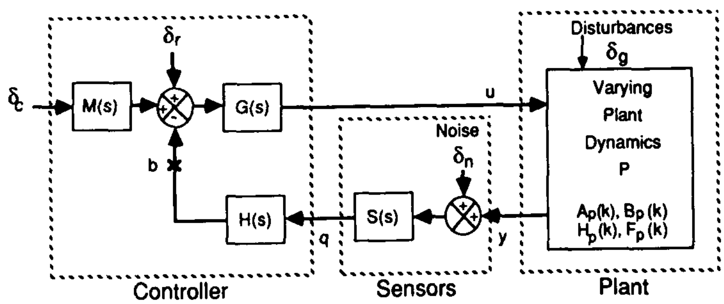

$$\begin{cases} \dot{x} = A(k)x + B(k)u \\ y = H(k)x + F(k)u \end{cases}$$

	Measurement	Constraint Frequency Response Loop Shaping
Stability	OLTF: $\frac{b}{\delta_r} \rightarrow \frac{b^1}{\delta_r^1} ; \frac{b^2}{\delta_r^2}$	Stability Margins/Forbidden Region (Each Loop, All PVs)
Performance	CLTF: $\frac{y}{\delta_c}$, $\frac{y}{\delta_g}$ $\rightarrow$ $\frac{Q,\ N_z,\ \alpha}{\text{STICK}}$; $\frac{P}{\text{ROLLSTK}}$; $\frac{N_y,\ \beta,\ R}{\text{RPEDAL}}$	CL Bode Response Boundary Envelopes (Each Constrained CLFR, All PVs) 1) Analytical Third-Order (or Reduced) Model 2) Table of Values (Mag, Phase vs ω)

Figure 2

OBJECTIVE FUNCTION (CLASSICAL VERSION)

The objective function for the classical version of the program, shown in figure 3, combines violations in stability (open-loop frequency responses (OLFR)) for each stability loop with violations in the magnitude/phase frequency responses of selected closed-loop scalar transfer functions, for all plant variations. Classical gain and phase margins (GM, PM) are used to define a Forbidden Region in the Nyquist/Nichols plane. This region is an area of uncertainty centered at the Nyquist critical point (-1, j0) or (0db, -180°) which the OLFR must avoid for adequate single input/single output (SISO) stability behavior. User-specified boundary constraints are imposed on the magnitude/phase closed-loop frequency responses (CLFR) which the actual CLFRs must be within to provide desirable performance.

$$J = J^{OL}_{Stability} + J^{CL}_{Performance}$$

$$J(p)_{Stab} = \sum_{PVs} \sum_{OLTFs} \sum_{\omega} f(\text{Stability Margins/Forbidden Region Violations})$$

$$J(p)_{Perf} = \sum_{PVs} \sum_{CLTFs} \sum_{\omega} f(\text{Magnitude/Phase Boundary Constraint Violations})$$

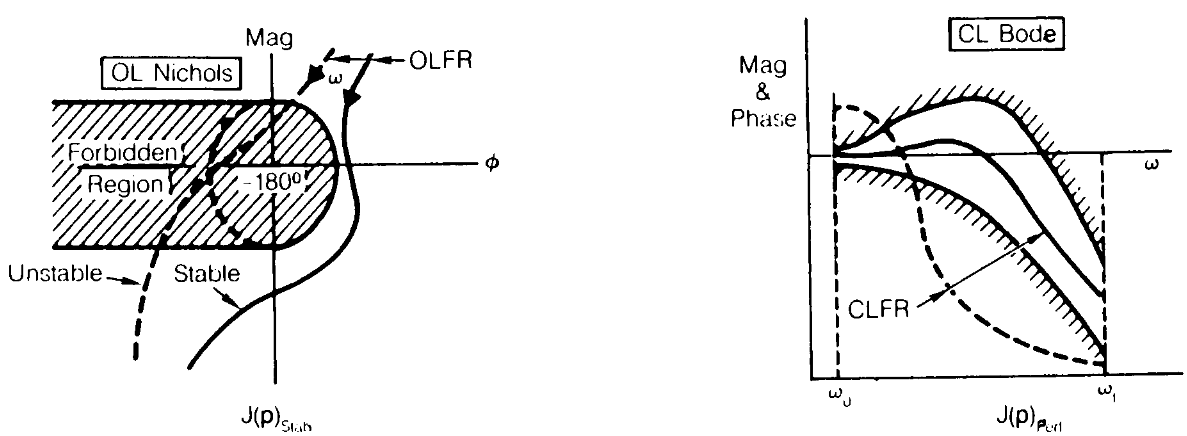

Figure 3

THE SEARCH ALGORITHM (NONLINEAR MATHEMATICAL PROGRAMMING)

A constrained local minimization procedure (Search Algorithm) is used to search for the active control parameters yielding minimum violation in all requirements considered collectively. The variable metric method of Davidson, Fletcher, and Powell (DFP Algorithm) (refs. 2,3) iteratively computes an approximation of the inverse Hessian matrix, H, which is used to deflect the gradient vector, $\nabla J(p) = \partial J/\partial p \approx \Delta J/\Delta p$, at a point in parameter hyperspace. The computation of this deflection matrix, η, $(\eta(p^i) \approx H^{-1}(p^i))$ hastens convergence since it is very effective in the vicinity of valleys in the hyperspace. The algorithm is also quite fast and not storage intensive since second partials need not be computed, nor must previous first or second derivatives be stored. The gradient is computed by a numerical perturbation procedure. A unidimensional search with quadratic interpolation is performed in the deflected gradient direction (search direction) to obtain the minimum in this direction. A gradient projection scheme is used to constrain the search within the feasible region. This is repeated for each search direction until the minimum is located. The iterative search algorithm is shown by the recursive equations and pictorially in figure 4.

- Constrained Local Minimization
  - DFP Algorithm
  - Unidimensional Search With Quadratic Interpolation
  - Gradient Projection

$$p^{i+1} = p^i - \lambda^{*i}\eta^i\,\nabla J(p^i),$$
$$p_{min} \leqslant p \leqslant p_{max}$$

$$\lambda^{*i} = J\left(p^i - \lambda^i\eta^i\,\nabla J(p^i)\right)_{min}$$

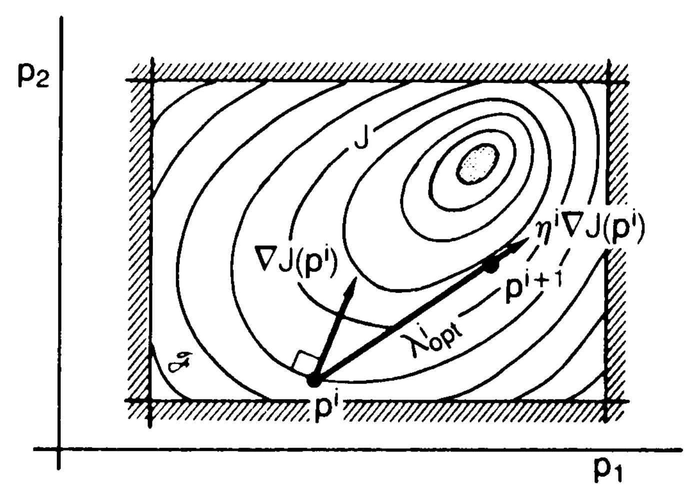

Figure 4

MIMO TRANSFER FUNCTION MATRICES DEFINITION

Shown below in figure 5 is a block diagram of a linear multivariable control system, subdivided into a controller, sensors and a plant. The representation here is of a plant with varying and uncertain plant dynamics given by the system matrices $A_p(k)$, $B_p(k)$, $H_p(k)$ and $F_p(k)$. The control system (controller and sensors) shown in Laplace transform notation can be combined with the plant state and output equations to form a total system state-space representation. It is convenient for multivariable systems to define certain matrix transfer functions. The loop transfer matrix, which depends upon the output node since matrix multiplication is not commutative, sensitivity matrix and complementary sensitivity matrix are defined in figure 5 (refs. 4,5).

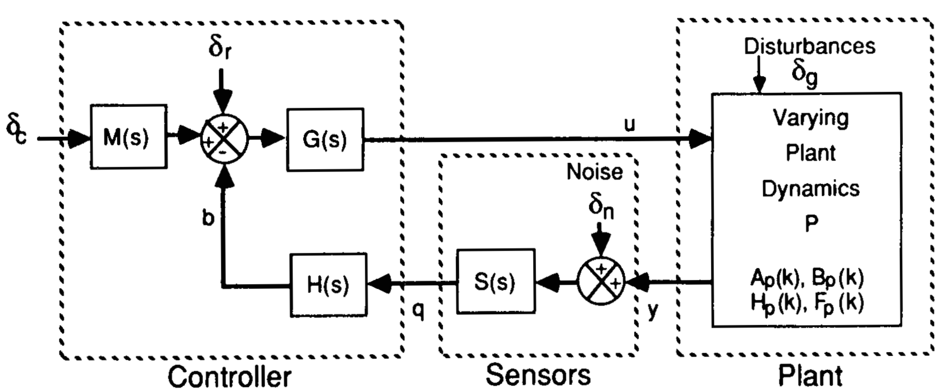

$$\begin{cases} \dot{x} = A(k)x + B(k)u \\ y = H(k)x + F(k)u \end{cases} \qquad P(k) = H(k)\,(Is - A(k))^{-1}\,B + F(k)$$

88-CSR-026-007

Loop Transfer Matrix $L(s) = L(\omega, \mathbf{p}) \triangleq P(s)\,G(s)\,H(s)\,S(s)$ at y node

$\triangleq G(s)\,H(s)\,S(s)\,P(s)$ at u node

Sensitivity Matrix $S(s) \triangleq (I + L(s))^{-1}$

Complementary Sensitivity Matrix $T(s) \triangleq I - S(s) = L(s)\,(I + L(s))^{-1}$

Figure 5

SINGULAR-VALUES DEFINITION

Nyquist stability theory, well founded and accepted for SISO systems, has been shown to be inadequate to describe robust MIMO system stability, because the determinant of the return difference matrix $(I + L(s))$ does not always provide a good indication of the proximity to singularity. Singular-values of a matrix A, $\sigma_i(A)$, however, provide a far better indication of system robustness since they provide a useful measure of the "size" of a matrix. Singular-values can be interpreted as the "gains" of a matrix for input vectors in various directions, as shown in figure 6 below. They also provide a natural extension to the familiar Bode frequency plots via the Bode sigma plot (Singular-values vs frequency). The singular-values of a matrix are defined as the nonnegative square roots of the eigenvalues $\lambda_i(A^H A)$, where A^H is the complex conjugate transpose of A. It is useful to define the maximum and minimum singular-values, $\bar{\sigma}(A)$ and $\underline{\sigma}(A)$, respectively. These will then form an upper and lower bound for $\sigma_i(A)$ on the Bode-sigma plot.

For Any Matrix A and Vector x

$$\sigma_i(A) \triangleq +\sqrt{\lambda_i(A^H A)}$$

$$\bar{\sigma}(A) \triangleq \max_i \sigma_i(A)$$

$$\underline{\sigma}(A) \triangleq \min_i \sigma_i(A)$$

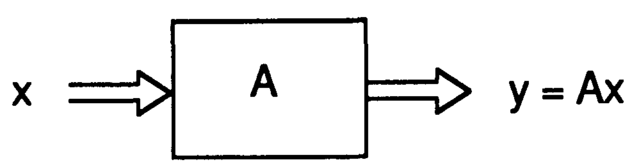

$$\bar{\sigma}(A) = \max_x \left(\frac{\|Ax\|}{\|x\|} \right) = \text{max gain of A}$$

$$\underline{\sigma}(A) = \min_x \left(\frac{\|Ax\|}{\|x\|} \right) = \text{min gain of A}$$

Figure 6

OBJECTIVE FUNCTION (MODERN ROBUSTNESS VERSION)

The objective function for the "modern" version of AUTOCON combines the MIMO robustness violation function $J_{robustness}$ with the "classical" version consisting of SISO stability and performance violation functions. The $J(p)_{robust}$ term considers violations in the user-defined singular-value constraints for each constrained matrix transfer function and for all plant variations. This is shown in figure 7 both with equations and graphically.

$$J = \left(J^{OL}_{Stability} + J^{CL}_{Performance} \right) + J_{Robustness}$$

$$J(p)_{Stab} = \sum_{PVs} \sum_{OLTFs} \sum_{\omega} f(\text{Stability Margins/Forbidden Region Violations})$$

$$J(p)_{Perf} = \sum_{PVs} \sum_{CLTFs} \sum_{\omega} f(\text{Magnitude/Phase Boundary Constraint Violations})$$

$$J(p)_{Robust} = \sum_{PVs} \sum_{TFMs} \sum_{\omega} f(\text{Singular-Value Constraint Violations})$$

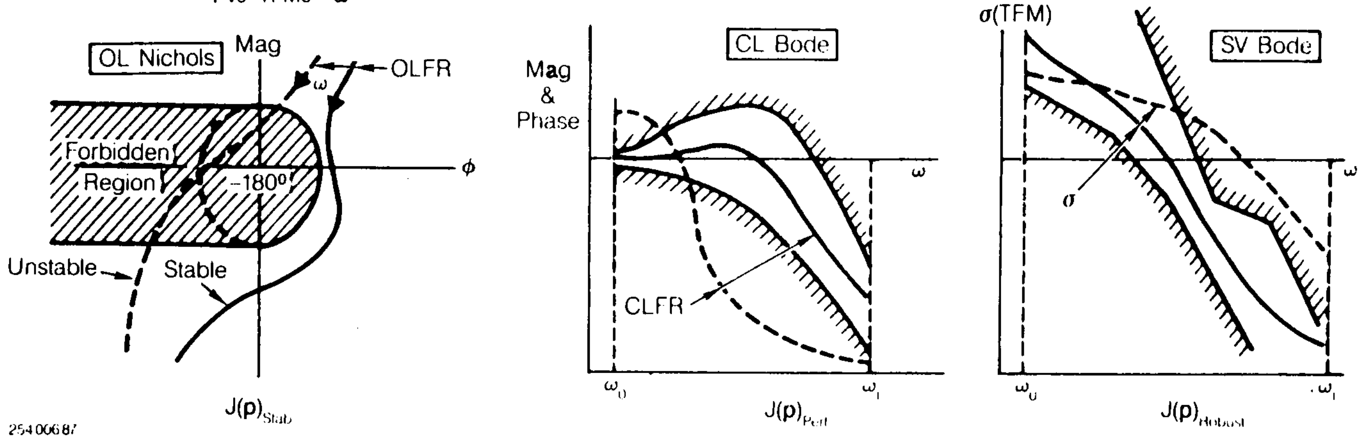

Figure 7

TYPICAL SINGULAR-VALUE BODE PLOTS AND SPECIFICATIONS

Typical singular-value frequency response (Bode) plots and constraints for a multivariable feedback control system are shown below in figure 8. The maximum singular-value plot of the sensitivity matrix $\bar{\sigma}(S)$ is constrained for disturbance attenuation and bandwidth in figure 8a, whereas, gain/phase margins (resonant peak) and unmodeled high frequency dynamics specifications are imposed on the maximum singular-value plot of the complementary sensitivity matrix $\bar{\sigma}(T)$ in figure 8b. Clearly, the singular-value frequency responses and specifications shown below are analogous to the usual SISO frequency responses and specifications. Connection between the resonant peaks M_T and M_S and classical gain/phase margins can be developed using the methods of references 6 and 7.

- Bandwidth & Disturbance Attenuation: $\bar{\sigma}$ (S)

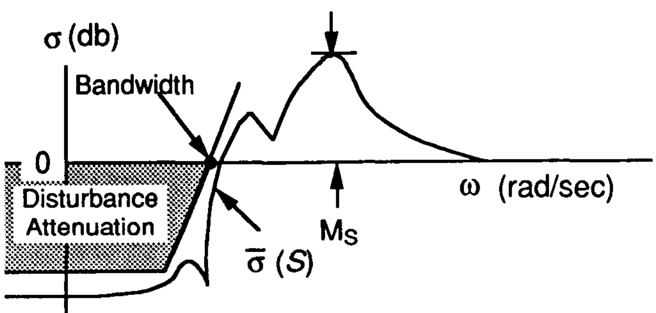

$$S \triangleq (I+L)^{-1}$$

$$T \triangleq L\,(I+L)^{-1}$$

(a)

- Gain / Phase Margin & Unmodeled High Frequency Dynamics : $\bar{\sigma}$ (T)

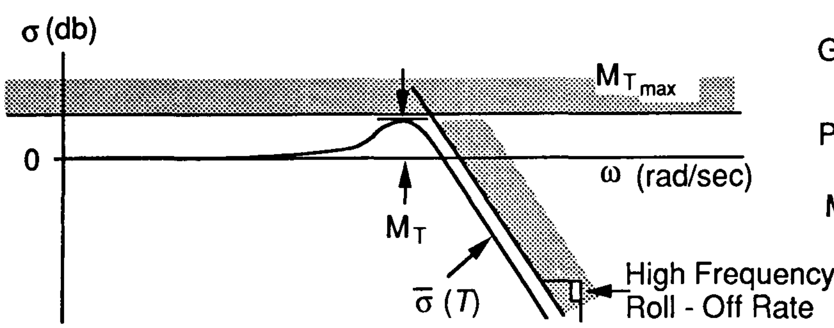

$$GM \geq \max\left[\left(\frac{1}{1-1/M_S}\right), \left(1+1/M_T\right)\right]$$

$$PM \geq 2\arcsin\left[\max\left(\frac{1}{2M_S}, \frac{1}{2M_T}\right)\right]$$

$$M_{T_{max}} = \left[2\sin\left(\frac{1}{2}PM_{spec}\right)\right]^{-1}$$

(b) Figure 8

AUTOCON DESIGN EXAMPLE

A design problem is presented below in figure 9 in which program AUTOCON is asked to synthesize a typical aircraft lateral/directional flight control system in which control of roll rate, P, and lateral acceleration Ny using the roll-stick and rudder pedal is effected, subject to combined MIMO robustness constraints and classical SISO stability and performance constraints, for three different operating points or flight conditions (plant variations). The synthesis and optimization will involve each constrained open- and closed-loop scalar and matrix transfer function for all plant variations, simultaneously. It is necessary for both the modern robustness constraints and the classical constraints to be active: 1) to ensure that the individual stability loops remain stable (closed-loop eigenvalues do not migrate into the right-half plane) and 2) to provide desirable SISO frequency response loop-shaping (classical specifications). The active control parameters chosen for this example were K_1, K_2, . . . K_9. In this design, K_1, K_2, K_4, and K_5 are scheduled (different gain value for each plant variation), while K_3, K_6, K_7, K_8, K_9 are nonscheduled (same value for each plant variation). This results in a total of 17 active control parameters.

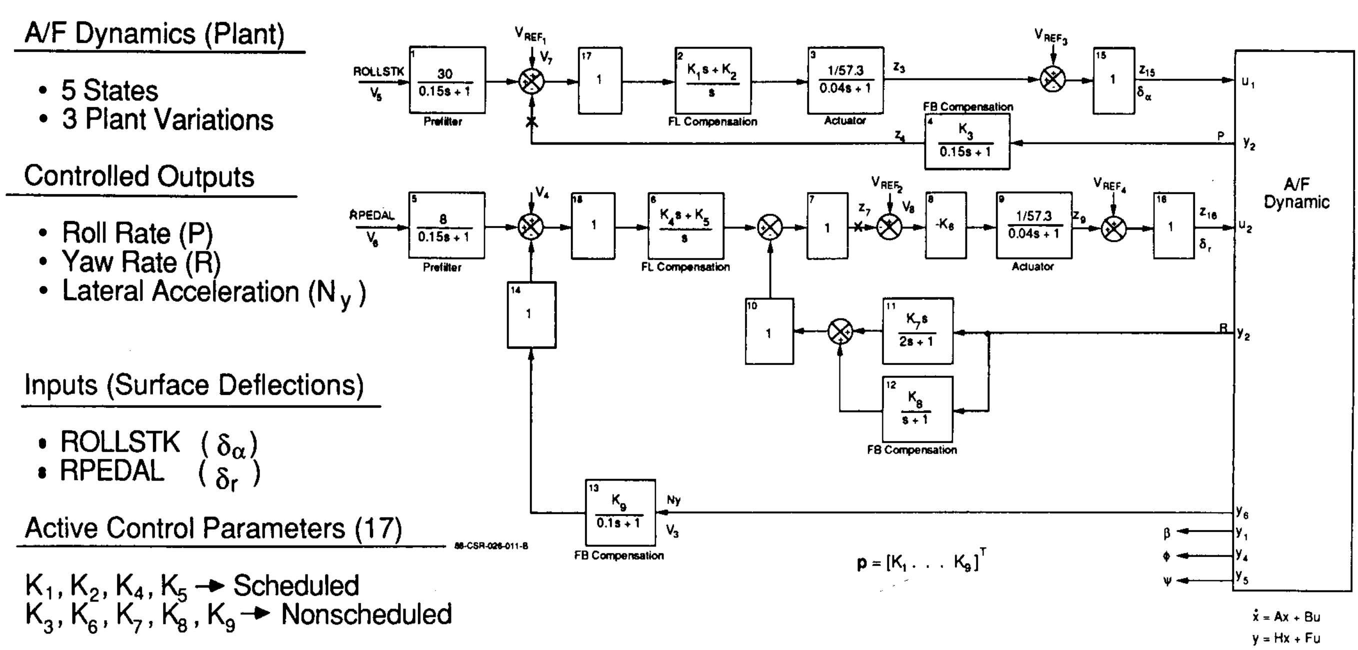

Figure 9

AUTOCON DESIGN EXAMPLE: SPECIFICATIONS

The classical SISO and modern MIMO robustness specifications for the AUTOCON design example are presented below in figure 10. Both the roll and yaw loops are desired to have at least 8 db of gain margin and 55 degrees of phase margin and each open-loop frequency response should not penetrate the Forbidden Region defined by the stability margins. It is also desired that the P/ROLLSTK response be within the performance bounds of an analytical 2nd- order model with parameters given below, with a steady-state value of 34 ± 0.4 db; and the Ny/RPEDAL response be within the performance bounds of a set of table values approximating a 2nd-order system with parameters given below, with a steady-state value of 11 ± 1.25 db. The robustness specifications include at least a 2 rad/sec system bandwidth, maximum disturbance attenuation and a $\bar{\sigma}(T)$ resonant peak less than or equal to 0.69 db (this provides at least 55 degrees phase margin and 8 db gain margin simultaneously in each loop).

SISO (Classical)

- Stability : Roll & Yaw Loops

$$\left.\begin{array}{l} GM \geq 8\text{ db} \\ PM \geq 55\text{ deg} \end{array}\right\} \begin{array}{c}\text{Forbidden}\\ \text{Region}\end{array}$$

- Performance:

P/ROLLSTK - 2nd Order Model ($\zeta = 0.8$, $4.0 \leq \omega_n \leq 6.0$ rad/sec)
Steady-State : 34 ± 0.4 db

N_y /RPEDAL - Table Values ($\zeta = 0.8$, $2.5 \leq \omega_n \leq 3.5$ rad/sec)
Steady-State : 11 ± 1.25 db

MIMO (Robustness)

$$\left.\begin{array}{l} \bullet\ \text{Bandwidth} \geq 2\text{ rad/sec} \\ \bullet\ \text{Maximize Disturbance Attentuation} \end{array}\right\} \bar{\sigma}(S)$$

- Stability Margins

$$M_T \leq 0.69\text{ db} \Rightarrow \left.\begin{array}{c} PM \geq 55\text{ deg} \\ GM \geq 8\text{db} \end{array}\right\} \left.\text{Simultaneously in each loop}\right\} \bar{\sigma}(T)$$

Figure 10

AUTOCON DESIGN EXAMPLE: PARAMETER CONSTRAINTS AND RESULTS

The admissible parameter range (linear inequality constraints) for the design problem is shown below in figure 11a. It is observed that the range for the forward-loop compensator parameters (scheduled) was selected as $.001 \le p \le 10.0$, whereas the remaining feedback parameter range (nonscheduled) was selected as $-10.0 \le p \le 10.0$. This was done to limit the forward-loop gains to positive values thereby preserving the sign convention, while allowing for possible feedback sign reversals from the nominal system shown in figure 9.

The results of the search, shown in figure 11b, indicate that a local minimum was found at a violation (J) of .0027. The effect of this violation is actually too small to be observed from the frequency responses presented in figures 12-15. The initial value chosen for all parameters was unity (no a priori information assumed). The final computer-generated scheduled and nonscheduled parameter values are also listed in figure 11b. It took 3.8 min on an IBM 3090 mainframe computer to synthesize this solution.

Active Parameter Constraints $P_{min} \le P \le P_{max}$

Parameter	K_1	K_2	K_3	K_4	K_5	K_6	K_7	K_8	K_9
P_{min}	0.001	0.001	-10.0	0.001	0.001	-10.0	-10.0	-10.0	-10.0
P_{max}	10.0								10.0

88-CSR-026-012

(a)

Results (J = .0027) CPU = 3.8 min (IBM 3090)

Scheduled Parameters

Parameter	K_1			K_2			K_4			K_5		
PV	1	2	3	1	2	3	1	2	3	1	2	3
Initial Value	1.0											1.0
Final Computer Generated Value	1.030	0.501	0.421	1.511	1.278	0.988	0.644	0.448	0.288	2.491	2.090	1.217

Nonscheduled Parameters

Parameter	K_3	K_6	K_7	K_8	K_9
Initial Value	1.0				1.0
Final Computer Generated Value	0.636	1.541	0.490	0.213	1.558

88-CSR-026-012A

(b)

Figure 11

AUTOCON DESIGN EXAMPLE: SISO NICHOLS PLOTS

The following pages contain the SISO and MIMO response plots of the airframe/control system with the unity initial control parameter values (before) and the system with the final computer-generated parameter values (after) for the three plant variations superimposed. The SISO open-loop frequency responses (Nichols plots) for the roll and yaw loops produced by AUTOCON are shown below in figure 12. The (8db, 55°) Forbidden Region (FR) is plotted as the closed broken contour (shaded). It is apparent from the initial roll loop responses in figure 12a that there is severe penetration into the FR for all three systems, violating the (8db, 55°)FR stability specification. As shown in figure 12c,d, SISO stability is adequate for the yaw loop. It is observed from figure 12b that AUTOCON has reshaped the roll loop Nichols responses around the FR by an adjustment of the active control parameters, the values of which are listed in Figure 11b.

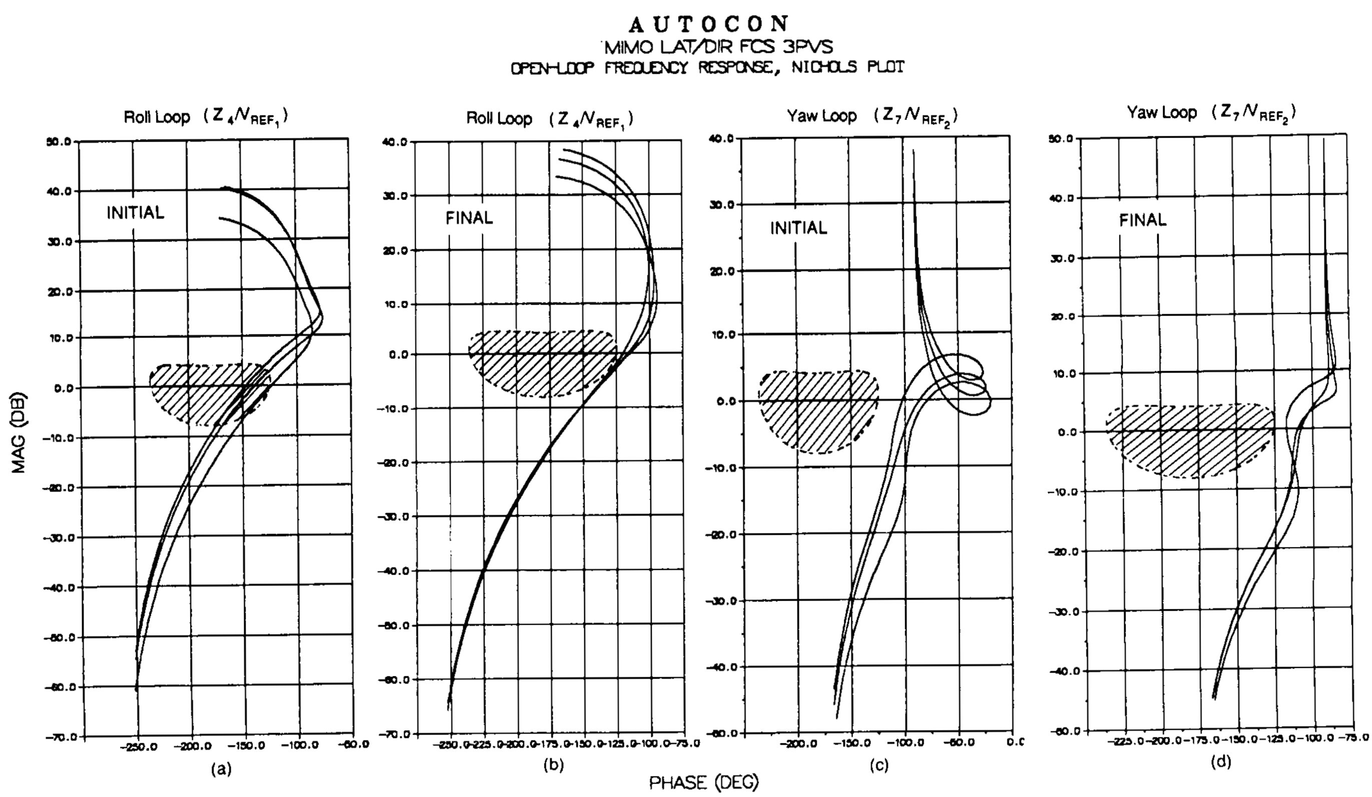

Figure 12

AUTOCON DESIGN EXAMPLE: SISO PERFORMANCE BODE RESPONSES

The SISO closed-loop Bode magnitude performance responses P/ROLLSTK and Ny/RPEDAL are presented below for the unity initial system in figure 13a,b and after the AUTOCON synthesis in figure 13c,d, respectively. The upper, lower and desired response boundary constraints consistent with the performance specifications given in figure 10 are shown as broken curves, with the unacceptable region shaded in figure 13. For this example, only the magnitude response was constrained. In general, magnitude and phase response constraints can be imposed. It is observed that there are severe violations for the unity initial parameter system both with respect to the steady-state values, shaping (notice the unacceptable resonance in the P/ROLLSTK response for two of the three plant variations), and sluggish Ny/RPEDAL responses. After the AUTOCON synthesis, the responses were forced into their respective boundaries, thereby satisfying the classical SISO specifications imposed on the system.

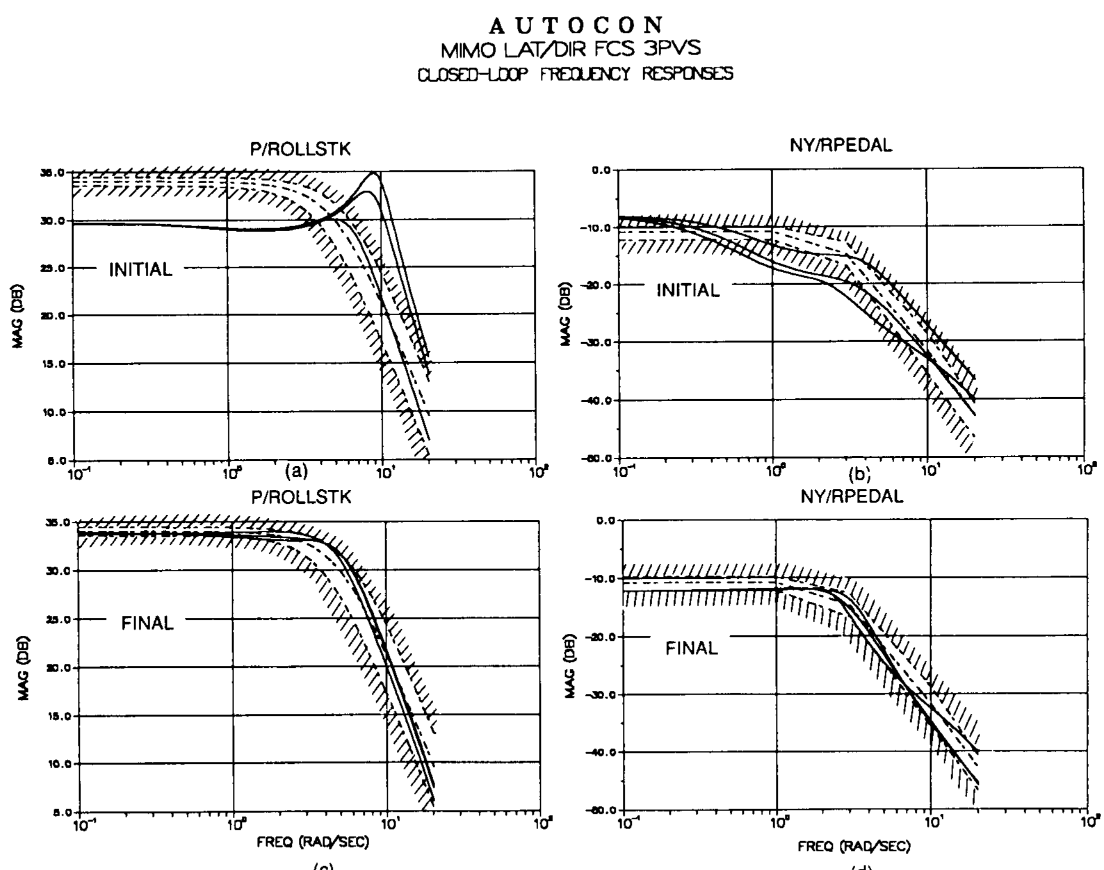

Figure 13

AUTOCON DESIGN EXAMPLE: MIMO SINGULAR-VALUE BODE RESPONSES

The singular-value sensitivity matrix and complementary sensitivity matrix Bode responses, $\sigma(S)$ and $\sigma(T)$, respectively, for the system with the unity initial parameter values and final computer-generated values are shown below in figure 14 for the three plant variations. Bandwidth, disturbance attenuation, gain/phase margin and unmodeled high-frequency roll-off specifications are drawn in figure 14 as broken boundary constraints with the unacceptable region shaded on the response plots. The $\sigma(S)$ and $\sigma(T)$ for this example are computed by AUTOCON from the MIMO matrix closed-loop transfer functions $(Z_{17}, Z_{18},)/V_{REF1}, V_{REF2})$ and $(Z_3, Z_4)/(V_{REF3}, V_{REF4})$ respectively. It is observed after comparing the initial and final sets of plots that AUTOCON successfully located a solution which satisfied the MIMO robustness specifications for all three plant variations, as given in figure 10. Note particularly the significant improvement in the disturbance attenuation for the $\bar{\sigma}(S)$ responses and the resonant peak magnitude M_T attenuation for the $\bar{\sigma}(T)$ responses. Satisfying the 0.69 db resonant peak magnitude constraint ensures at least 55 degrees phase margin in each loop even when the variations occur simultaneously in both loops. At least 8 db gain margin in each loop is also obtained by virtue of the equations shown in figure 8b.

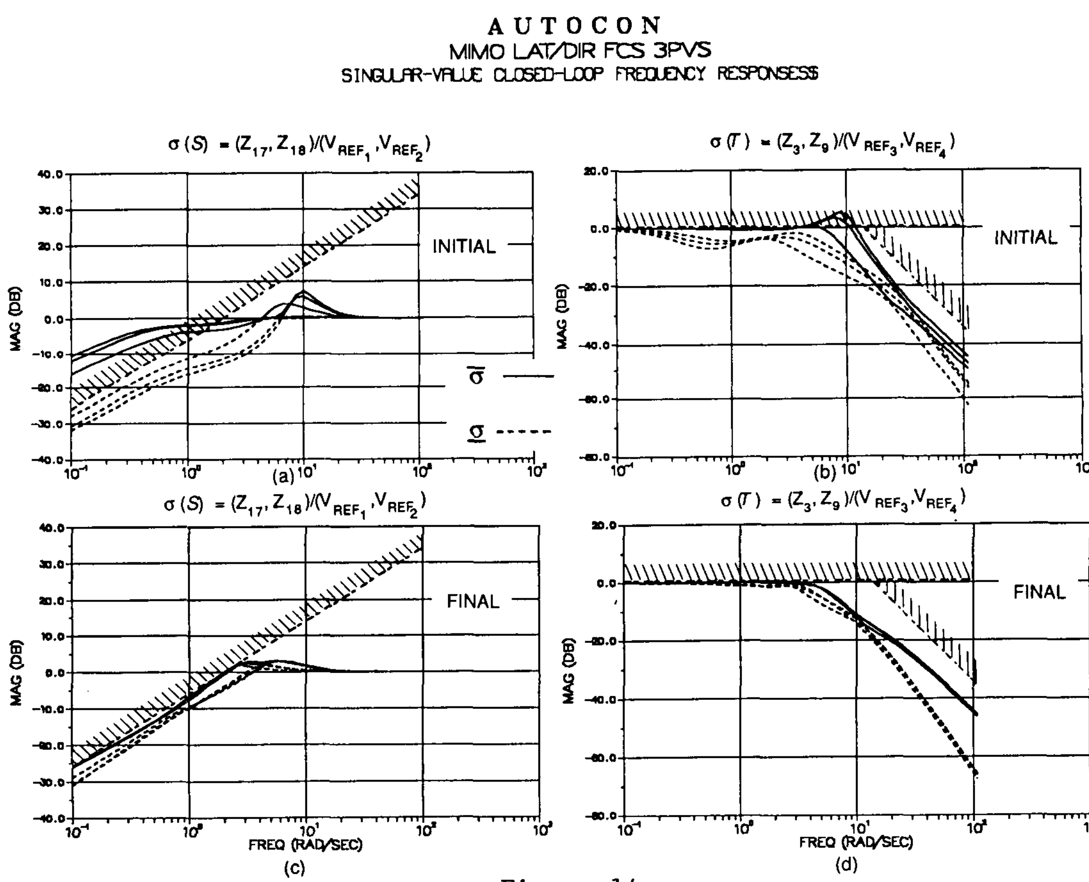

Figure 14

AUTOCON DESIGN EXAMPLE: TRANSIENT RESPONSES

Finally, transient responses of the constrained outputs roll rate, P, and lateral acceleration, Ny, to unit step ROLLSTK and RPEDAL input commands, respectively, are produced and shown below in figure 15 before and after the AUTOCON synthesis and optimization, for the systems with the three plant variations. Comparing the initial and final system P responses (figure 15a,b) shows that the poor initial responses (improper steady-state value and ringing) has been corrected by the optimization process and now satisfies the specifications. The upper, lower and desired transient boundary responses (broken curves) were computed from the second-order model parameters (specification) given in figure 10 and superimposed on the system transient responses. The shaded area indicates undesirable response regions. Objective function violations are measured in AUTOCON in the frequency-domain and not in the time-domain (transfer functions provide for a better more general measure for this application since they are not input dependent). Therefore, there may be some minor differences when comparing the two domains with respect to excursions from the desired response region. Since sets of table values were used to define the Ny/RPEDAL performance boundary constraints (note the sharp break-points in the broken boundary curves in figure 13b,d) exact 2nd order parameter values are unknown, and therefore, overlay boundary responses are not provided for the Ny transient response. Notice, however, how well the sluggish initial system Ny responses (figure 11c) were improved by the program (figure 15d). It is important to understand that all SISO "classical" and MIMO robustness specifications and constraints imposed for this AUTOCON design problem were active simultaneously in the search for an optimum solution and were satisfied by the final computer-generated values. The solution was obtained in only one computer run.

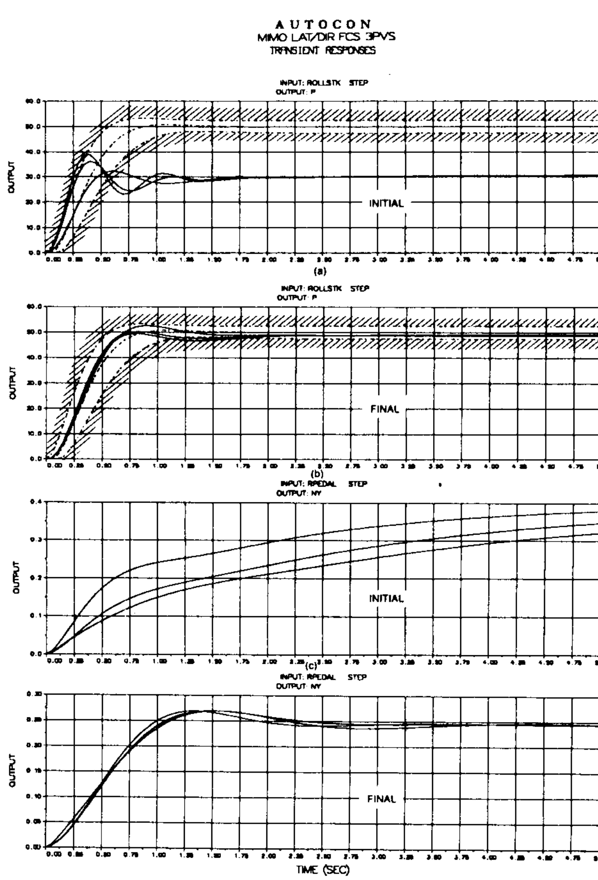

Figure 15

CONCLUSION

The automated computer-aided design tool, AUTOCON, used for the synthesis and optimization of linear control systems has been expanded to handle robust multivariable constraints in addition to the "classical" single-input/single-output stability and performance requirements. The synthesis and optimization can be performed on systems with fixed plant dynamics as well as those with varying dynamics. AUTOCON thereby enables the designer to combine classical SISO and modern MIMO control system stability/performance specifications within a highly flexible nonlinear programming design optimization environment.

The classical version of AUTOCON was first reviewed, followed by an introduction of the new multivariable robustness version of the program. Basic multivariable robustness concepts involving singular-values were discussed and an automated computer design example using AUTOCON was presented.

REFERENCES

1. Lefkowitz, C.P.: AUTOCON Version 3.0, User's Manual. Northrop Corp., March, 1987.

2. Davidon, W.C.: Variable Metric Method for Minimization. Argonne National Laboratory Report ANL-5990, November, 1959, revised February 1966.

3. Fletcher, R.; and Powell, M.J.D.: A Rapidly Convergent Descent Method for Minimization. Computer J. Vol. 6, pp. 163-168, 1963.

4. Safonov, M.G.; Laub, A.J.; and Hartmann, G.L.: Feedback Properties of Multivariable Systems: The Role and Use of the Return Difference Matrix. IEEE Trans. Auto. Contr., Vol. AC-26, pp. 47-65, February, 1981.

5. Doyle, J.C; and Stein, G.: Multivariable Feedback Design: Concepts for a Classical/Modern Synthesis. IEEE Trans. Auto. Contr., Vol. AC-26, pp. 4-16, February, 1981.

6. Safonov, M.G.; and Athans, M.: Gain and Phase Margin for Multiloop LQG Regulators. IEEE Trans. Auto. Contr., Vol. AC-22, pp. 173-179, April 1977.

7. Lehtomaki, N.A.; Sandell, N.R., Jr.; an Athans, M.: Robustness Results in Linear-Quadratic Gaussian Based Multivariable Control Designs. IEEE Trans Auto. Contr., Vol. AC-26, pp. 75-92, February 1981.